Electronic Supplementary Material (ESI) for Nanoscale.

Supporting Information

Bimetallic RuNi-Decorated Mg-CUK-1 for Oxygen-Tolerant Carbon Capture and Conversion to Methane

Timothy Zurrer, Emma Lovell, Zhaojun Han, Kang Liang, Jason Scott, Rose Amal**

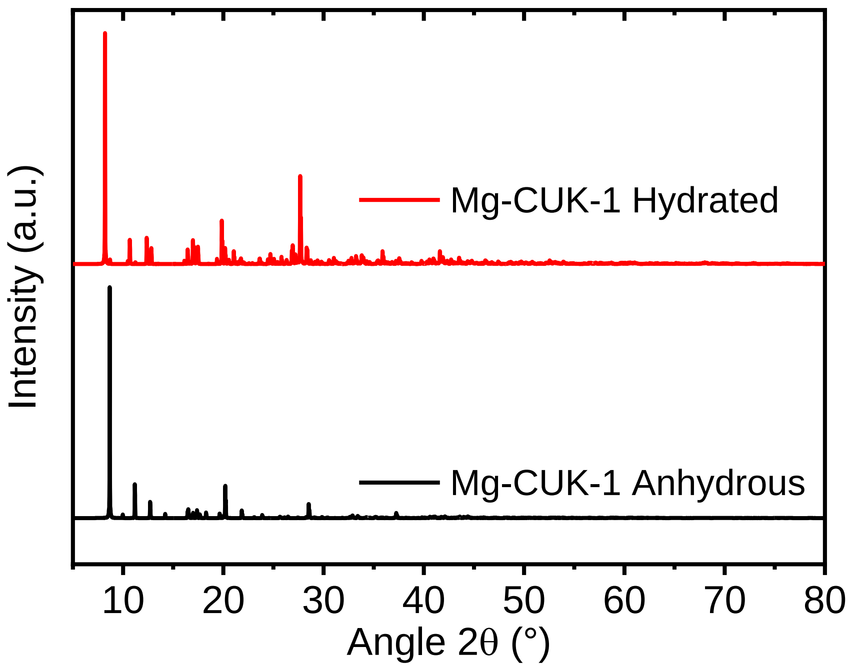

Figure S1. Simulated powder XRD patterns for Mg-CUK-1 under anhydrous and hydrated conditions.

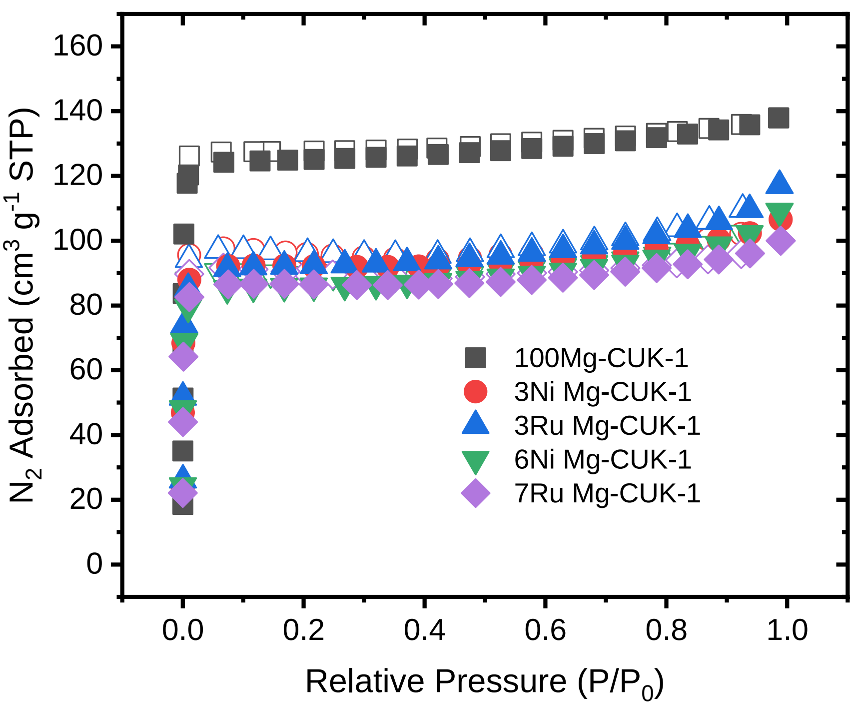

Figure S2. N_2 adsorption isotherms of Mg-CUK-1 before and after loading with Ni and Ru.

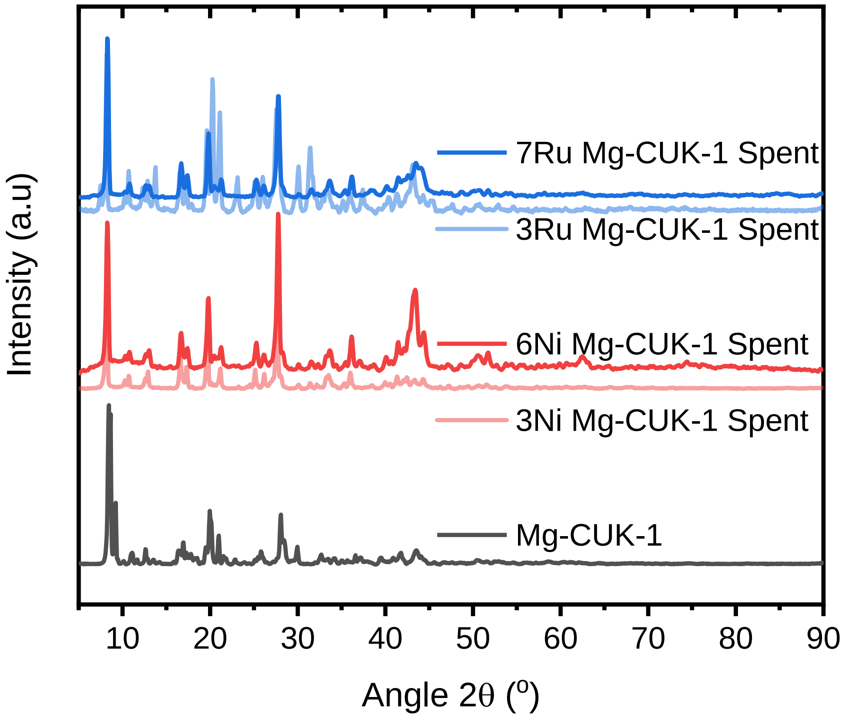

Figure S3. X-ray diffraction patterns of spent Ni- and Ru-loaded Mg-CUK-1 following steady state CO_2 hydrogenation performance tests.

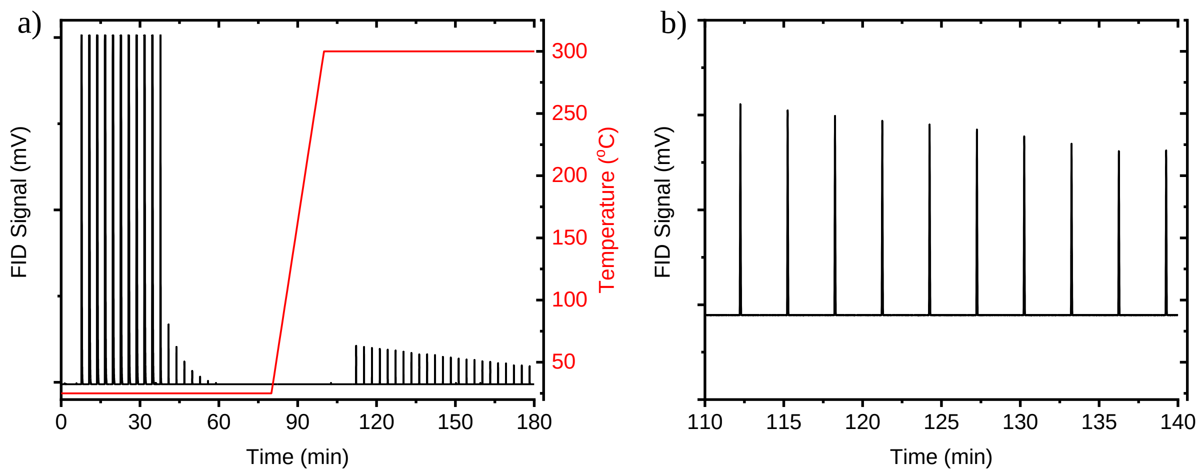

Figure S4. Representative gas chromatograph flame ionization detector (GC-FID) signal for the CO_2 capture and conversion experimental runs. a) Complete experimental time on stream data and b) first 10 peaks associated with CH_4 generation.

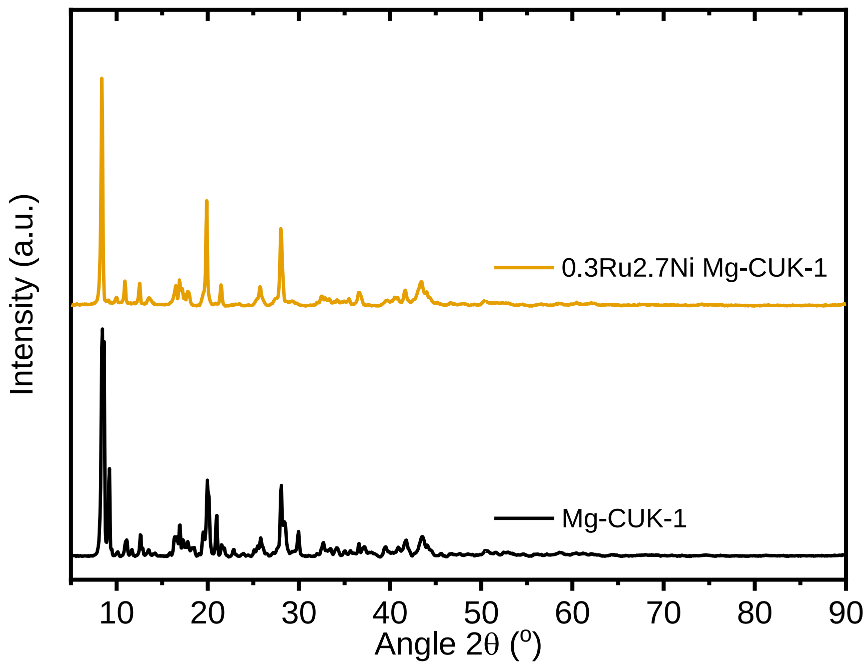

Figure S5. X-ray diffraction patterns of 0.3Ru2.7Ni-loaded Mg-CUK-1. Neat Mg-CUK-1 is provided for comparison.

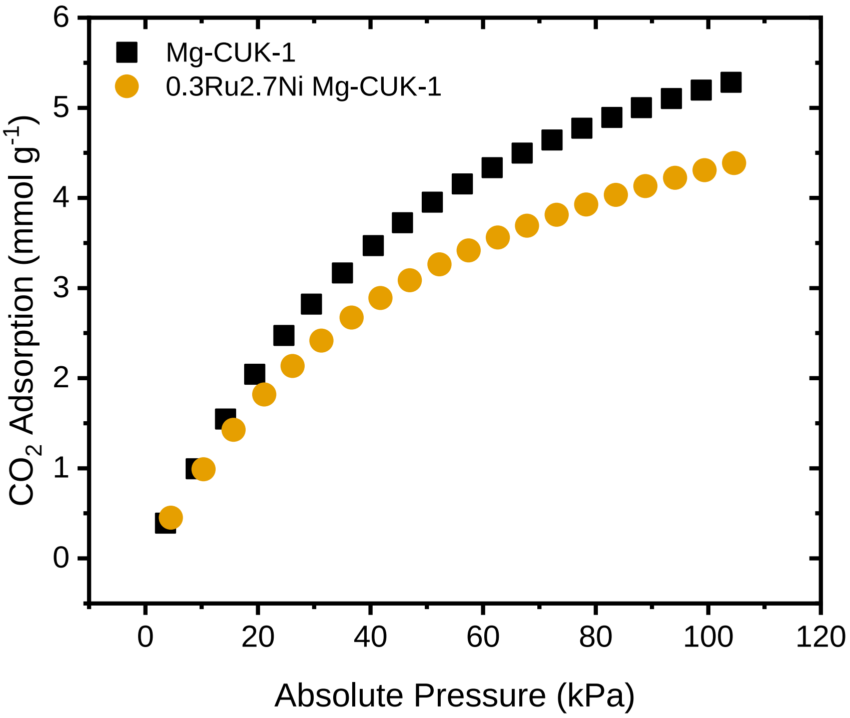

Figure S6. CO_2 adsorption isotherm of 0.3Ru2.7Ni Mg-CUK-1. Neat Mg-CUK-1 is provided for comparison

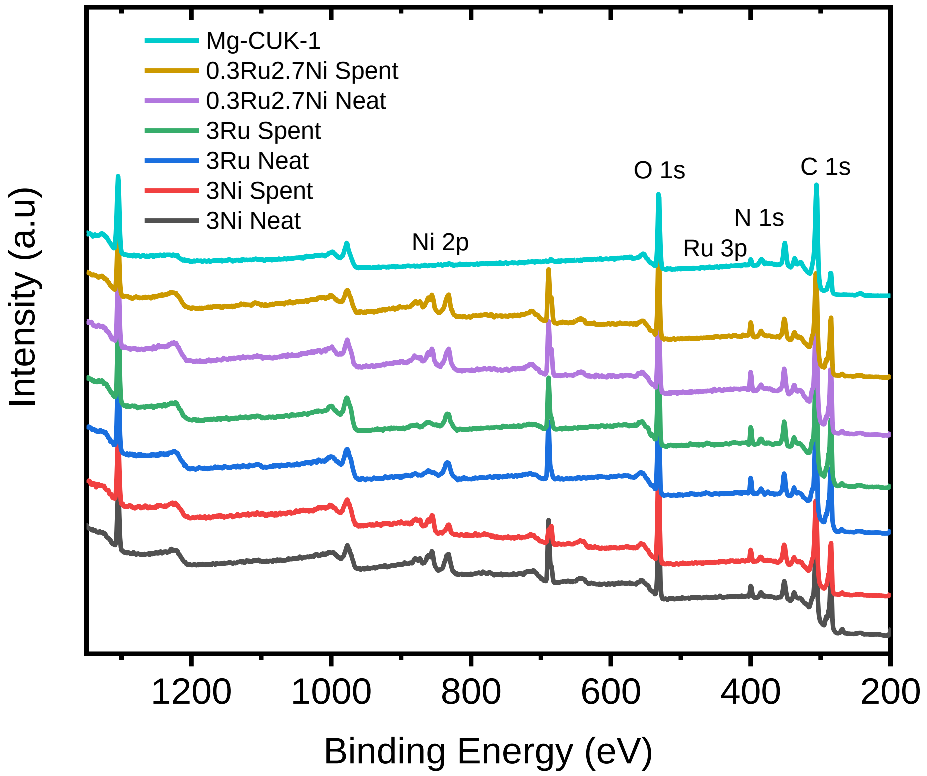

Figure S7. Survey XPS spectra of Mg-CUK-1 before and loading with Ni and Ru.

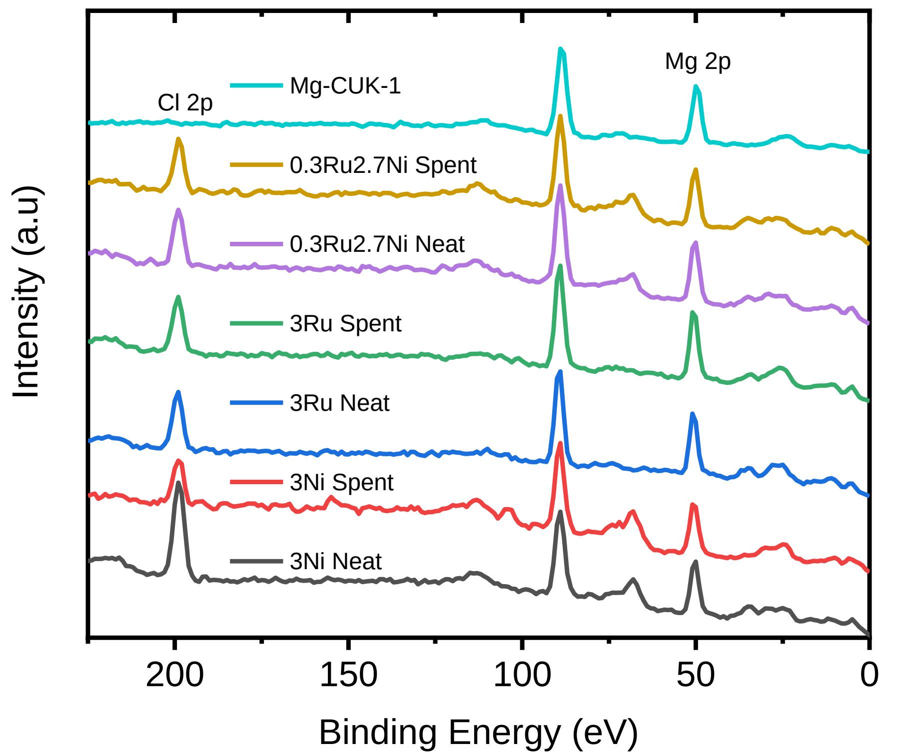

Figure S8. Survey XPS spectra of Mg-CUK-1 below 200 eV binding energy before and after loading with Ni and Ru.

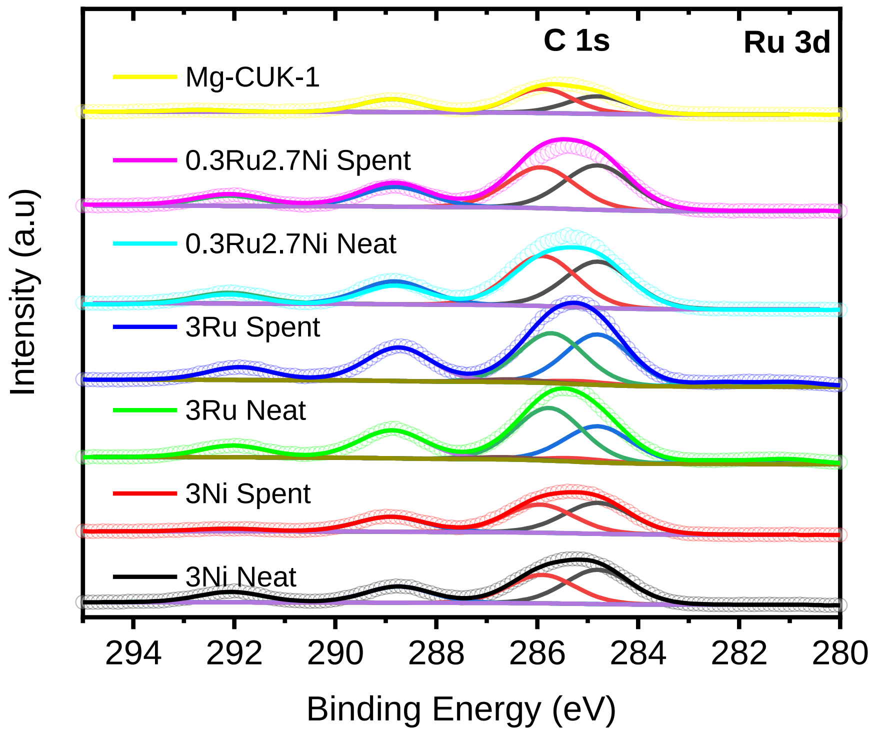

Figure S9. High-resolution XPS spectra for the C 1s and Ru 3d region of Mg-CUK-1 before and loading with Ni and Ru.

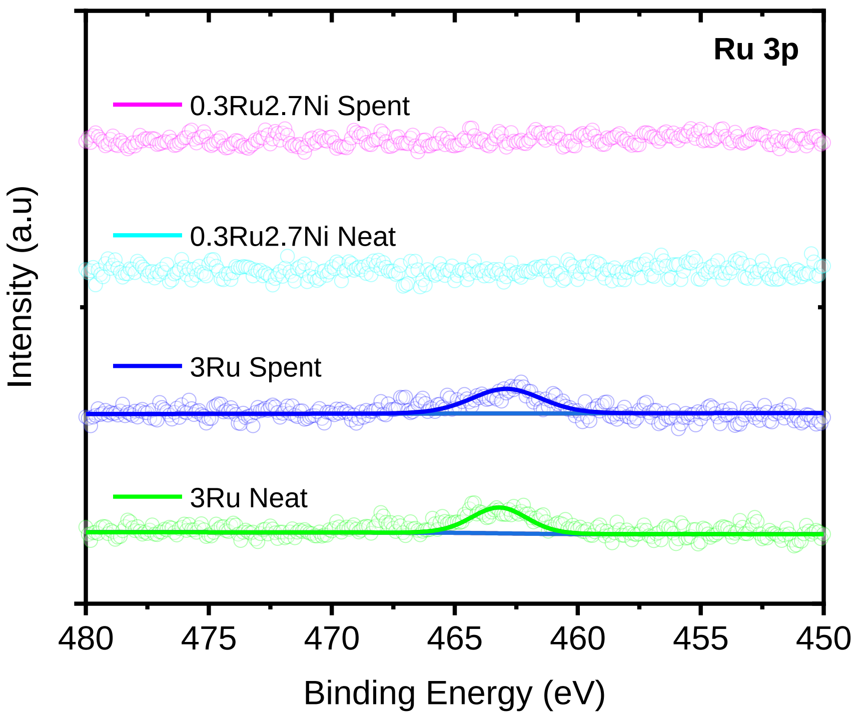

Figure S10. High-resolution XPS spectra for the Ru 3p region of Mg-CUK-1 before and loading with Ni and Ru.

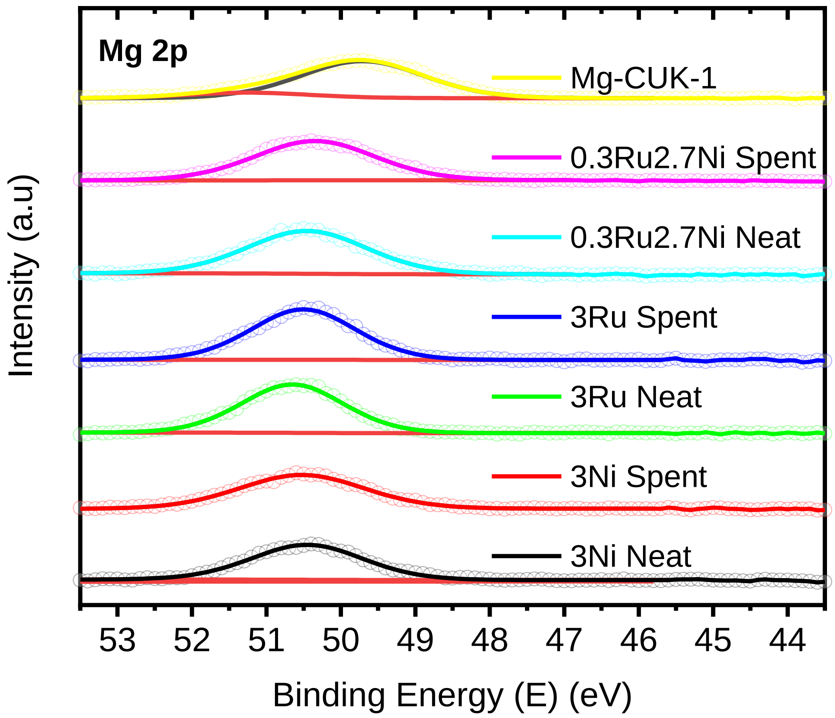

Figure S11. High-resolution XPS spectra for the Mg 2p region of Mg-CUK-1 before and loading with Ni and Ru.

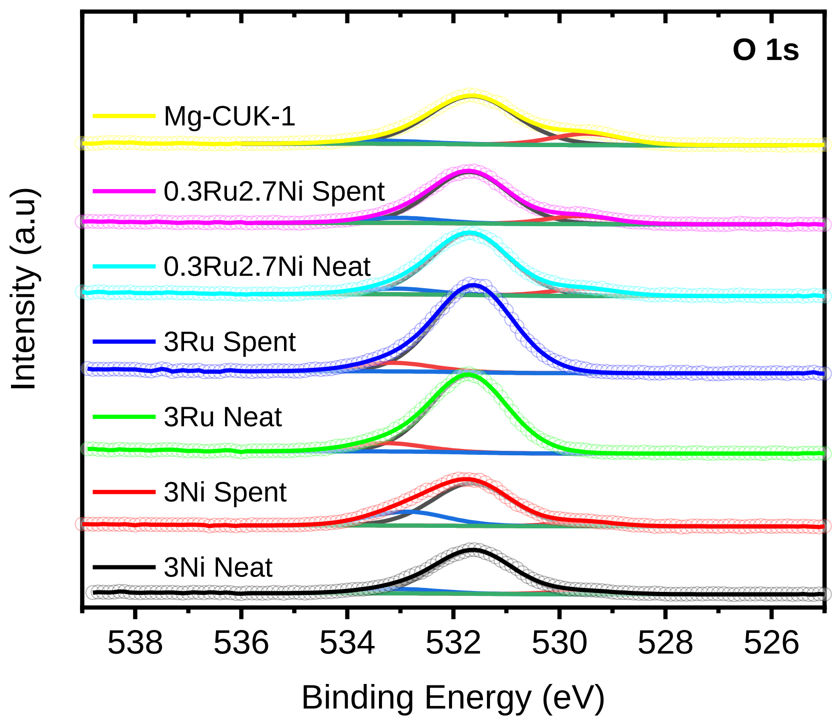

Figure S12. High-resolution XPS spectra for the O 1s region of Mg-CUK-1 before and loading with Ni and Ru.

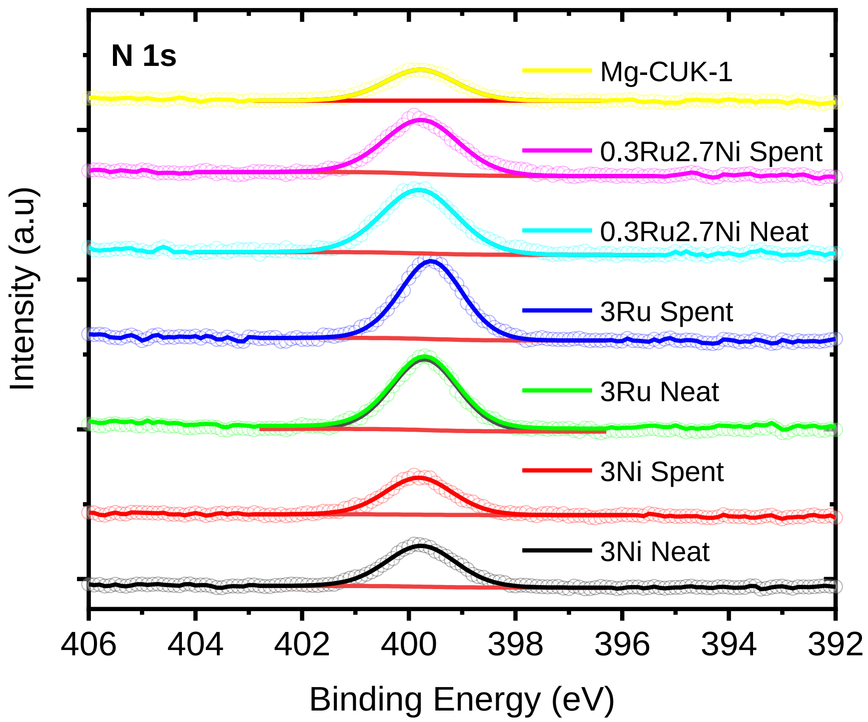

Figure S13. High-resolution XPS spectra for the N 1s region of Mg-CUK-1 before and loading with Ni and Ru.

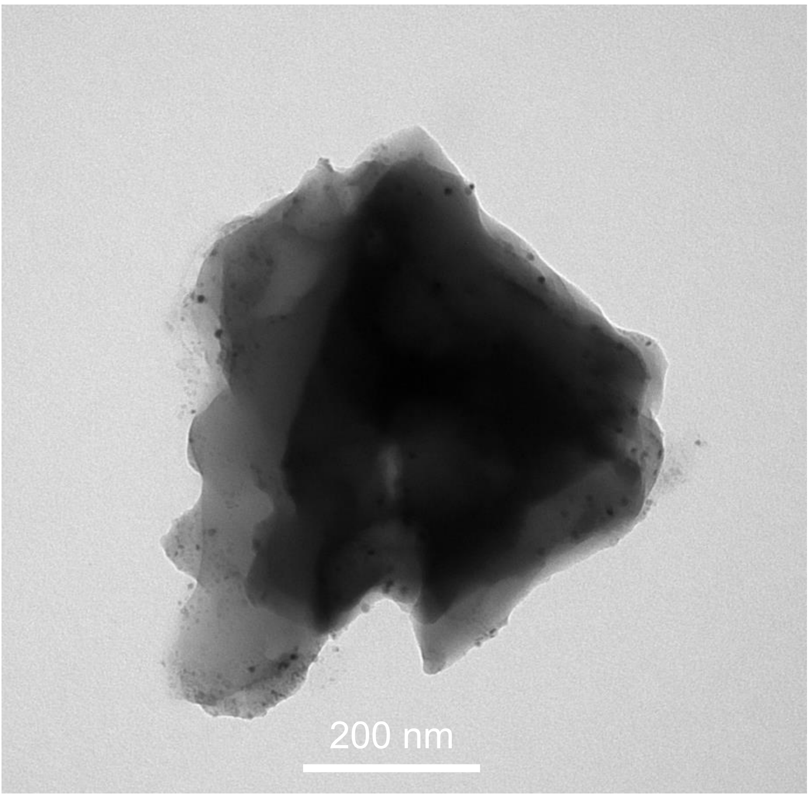

Figure S14. Transmission electron micrograph of 0.3Ru2.7Ni Mg-CUK-1.

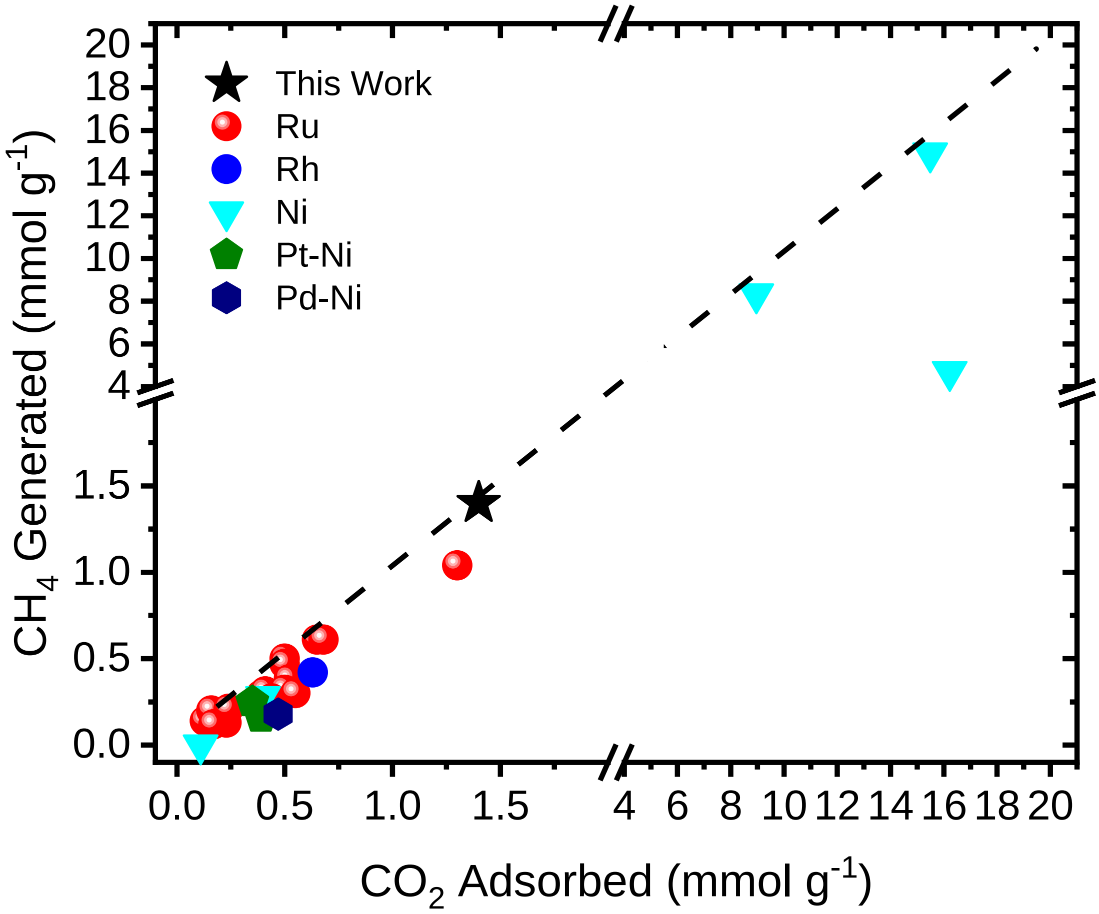

Figure S15. Comparison of previous hybrid sorbent/catalyst isothermal reactor systems for carbon capture and conversion to methane using metal oxide/carbonate CO_2 sorbents with present work (0.3Ru2.7Ni Mg-CUK-1) under temperature-swing conditions. Data is sorted based on included metal catalyst. Dashed line represents parity between CO_2 uptake and CH_4 generation indicating complete CO_2 utilisation. It is important to mention that all but two of the literature performance data included for comparison were conducted under isothermal conditions. The work reported here uses a temperature-swing operation to maximise CO_2 uptake at room temperature in the physisorption-based sorbent, Mg-CUK-1, before hydrogenation at 300 °C. Further details regarding the reported literature can be found in Table S6.

Table S1. Physicochemical properties of Ni- and Ru-loaded Mg-CUK-1. CO_2 Uptake at 0 °C, 104.9 kPa, BET surface area calculated from N_2 adsorption/desorption isotherms collected at -196.15 °C and catalyst loading obtained from ICP-OES.

Sample	CO_2 Uptake (mmol g^{-1})	BET surface area (m^2 g^{-1})	Catalyst Loading (wt%)
Mg-CUK-1	5.28	542.3 ± 4.4	-
3Ni Mg-CUK-1	4.41	389.7 ± 4.1	3.10
3Ru Mg-CUK-1	4.11	386.7 ± 7.5	3.41
6Ni Mg-CUK-1	4.07	365.9 ± 3.8	6.22
7Ru Mg-CUK-1	3.76	360.1 ± 7.0	7.40
0.3Ru2.7Ni Mg-CUK-1	4.39	387.2 ± 4.0	0.34 (Ru) 2.73 (Ni)

Table S2. Possible reaction pathways governing the catalytic thermal hydrogenation of CO_2

Reaction Name	Reaction Formula	ΔH_{298K} [kJ mol^{-1}]	
CO_2 methanation (Sabatier) reaction	$CO_2 + 4H_2 \rightleftharpoons CH_4 + 2H_2O$	-165	1
Reverse water-gas shift	$CO_2 + H_2 \rightleftharpoons CO + H_2O$	41	2
CO methanation	$CO + 3H_2 \rightleftharpoons CH_4 + H_2O$	-206	3

Table S3. Binding energy of peak positions for Ni 2p region of 3Ni- and 0.3Ru2.7Ni-loaded Mg-CUK-1 before (neat) and after ten carbon capture and conversion performance tests (spent).

Sample	**Ni A (Ni^0)**	**Ni B**	**Ni D**	**Ni E**
3Ni Neat	853.48	855.47	860.99	863.97
3Ni Spent	-	855.35	861.52	864.15
0.3Ru2.7Ni Neat	853.75	855.64	861.37	863.81
0.3Ru2.7Ni Spent	853.31	855.15	860.93	862.42

Table S4. Peak area percentage for Ni 2p region of 3Ni- and 0.3Ru2.7Ni-loaded Mg-CUK-1 before (neat) and after ten carbon capture and conversion performance tests (spent) illustrating shift to lower binding energies.

Sample	Ni A (Ni^0)	Ni B	Ni D	Ni E
3Ni Neat	18.04	48.56	27.62	5.78
3Ni Spent	0	59.46	31.84	8.7
0.3Ru2.7Ni Neat	18.58	47.61	27.67	6.14
0.3Ru2.7Ni Spent	16.54	53.47	18.15	11.84

Table S5. Comparison of Ni $2p_{3/2}$ peak areas as an approximation of the ratio of Ni^{2+} reduced to Ni^0 for 3Ni- and 0.3Ru2.7Ni-loaded Mg-CUK-1 before (neat) and after ten carbon capture and conversion performance tests (spent).

Sample	Ni^0 (853 eV)	Ni^{2+} (855 eV)
3Ni Neat	27.09%	72.91%
3Ni Spent	0%	100%
0.3Ru2.7Ni Neat	28.07%	71.93%
0.3Ru2.7Ni Spent	23.63%	76.37%

Table S6. Summary of literature studies involving dual functional materials for combined CO_2 capture and methanation

Dual Functional Material	CO_2 Adsorption		CH_4 generation		Ref
Catalyst-Sorbent-Support	Operation Conditions	Adsorption capacity (mmol CO_2 g^{-1})	Operation Conditions	Production capacity (mmol CH_4 g^{-1})	
0.3Ru2.7Ni Mg-CUK-1	15%CO_2/Air, 25 °C, 1 h	1.37-1.40	100% H_2, 300 °C, 10 min	1.37-1.40	This Work
1%Ru-10%"Na_2O"/γ-Al_2O_3	400 ppm CO_2/Air, 25 °C, >2 h (Dry Air)	0.55	15% H_2/N_2, 300 °C, 2 h	0.3	[1]
1%Ru-10%"Na_2O"/γ-Al_2O_3	400 ppm CO_2/Air, 25 °C, >4 h (Humid Air; ~ 2% H_2O, 90% RH)	1.3	15% H_2/N_2, 300 °C, 2 h	1.04	[1]
5%Ru-6.1%Na_2O/γ-Al_2O_3 (tablets)	7.5% CO_2/N_2, 320 °C, 30 min	0.40	5% H_2/N_2, 320 °C, 30 min	0.24	[2]
5%Ru-10%CaO/ γ-Al_2O_3	10% CO_2/N_2, 320 °C, 30 min	0.41	4% H_2/N_2, 320 °C, 2 h	0.31	[3]
5%Ru-10%CaO/Al_2O_3 tableted powder (BASF)	7.5% CO_2, 15% H_2O, 4.5% O_2, 73% N_2, 320 °C, 20 min	0.23	5% H_2/N_2, 320 °C, 60 min	0.13	[4]

5%Ru-10%CaO/Al_2O_3 Pellets (TH200)	7.5% CO_2, 15% H_2O, 4.5% O_2, 73% N_2, 320 °C, 20 min	0.13	5% H_2/N_2, 320 °C, 60 min	0.14	[4]
5%Ru-10%CaO/Al_2O_3 Pellets (TH100)	7.5% CO_2, 15% H_2O, 4.5% O_2, 73% N_2, 320 °C, 20 min	0.16	5% H_2/N_2, 320 °C, 60 min	0.20	[4]
5%Ru-10%CaO/Al_2O_3 Pellets (SAS200)	7.5% CO_2, 15% H_2O, 4.5% O_2, 73% N_2, 320 °C, 20 min	0.17	5% H_2/N_2, 320 °C, 60 min	0.12	[4]
5%Ru-10%CaO/Al_2O_3	10% CO_2/N_2, 320 °C, 30 min	-	4% H_2/N_2, 320 °C, 2 h	0.50	[5]
5%Ru-10%K_2CO_3/Al_2O_3	10% CO_2/N_2, 320 °C, 30 min	-	4% H_2/N_2, 320 °C, 2 h	0.91	[5]
5%Ru-10%Na_2CO_3/Al_2O_3	10% CO_2/N_2, 320 °C, 30 min	-	4% H_2/N_2, 320 °C, 2 h	1.05	[5]
5%Ru-10%Na_2CO_3/Al_2O_3	5% CO_2/N_2, 320 °C, 30 min	0.52	2% H_2/N_2, 320 °C, 30 min	0.39	[5]
10%Ni-6.1%"Na_2O"/Al_2O_3 (1g)	7.5% CO_2/N_2, 320 °C, 30 min	0.40	15% H_2/N_2, 320 °C, 1 h	0.28	[6]
10%Ni-6.1%"Na_2O"/Al_2O_3 (1g)	7.5% CO_2, 4.5% O_2, 15% H_2O, 73% N_2, 320 °C, 20 min	0.11	15% H_2/N_2, 320 °C, 1 h	0	[6]
5%Ru-6.1%"Na_2O"/Al_2O_3 (0.1g)	7.5% CO_2, 4.5% O_2, 15% H_2O, 73% N_2, 320 °C, 20 min	0.39	15% H_2/N_2, 320 °C, 1 h	0.29	[6]

5%Ru-6.1%"Na_2O"/Al_2O_3	10% CO_2/N_2, 320 °C, 30 min	0.65	10% H_2/N_2, 320 °C, 1 h	0.61	[6]
0.5%Rh-6.1%"Na_2O"/Al_2O_3	10% CO_2/N_2, 320 °C, 30 min	0.63	10% H_2/N_2, 320 °C, 1 h	0.42	[6]
5%Ru-7.01%"K_2O"/Al_2O_3	10% CO_2/N_2, 320 °C, 30 min	0.50	10% H_2/N_2, 320 °C, 1 h	0.47	[6]
5%Ru-10%CaO/Al_2O_3	10% CO_2/N_2, 320 °C, 30 min	0.68	10% H_2/N_2, 320 °C, 1 h	0.61	[6]
5%Ru-10%MgO/Al_2O_3	10% CO_2/N_2, 320 °C, 30 min	0.24	10% H_2/N_2, 320 °C, 1 h	0.21	[6]
1%Ru-10%Ni-6.1%"Na_2O"/Al_2O_3	7.5% CO_2, 4.5% O_2, 15% H_2O, 73% N_2, 320 °C, 20 min	0.52	15% H_2/N_2, 320 °C, 1 h	0.38	[7]
1%Ru-6.1%"Na_2O"/Al_2O_3	7.5% CO_2, 4.5% O_2, 15% H_2O, 73% N_2, 320 °C, 20 min	0.41	15% H_2/N_2, 320 °C, 1 h	0.31	[7]
0.1%Ru-10%Ni-6.1%"Na_2O"/Al_2O_3	7.5% CO_2, 4.5% O_2, 15% H_2O, 73% N_2, 320 °C, 20 min	0.50	15% H_2/N_2, 320 °C, 1 h	0.32	[7]
0.1%Ru-6.1%"Na_2O"/Al_2O_3	7.5% CO_2, 4.5% O_2, 15% H_2O, 73% N_2, 320 °C, 20 min	0.44	15% H_2/N_2, 320 °C, 1 h	0.27	[7]
0.1%Pt-10%Ni-6.1%"Na_2O"/Al_2O_3	7.5% CO_2, 4.5% O_2, 15% H_2O, 73% N_2, 320 °C, 20 min	0.39	15% H_2/N_2, 320 °C, 1 h	0.16	[7]

1%Pt-10%Ni-6.1%"Na_2O"/Al_2O_3	7.5% CO_2, 4.5% O_2, 15% H_2O, 73% N_2, 320 °C, 20 min	0.35	15% H_2/N_2, 320 °C, 1 h	0.25	[7]
0.1%Pd-10%Ni-6.1%"Na_2O"/Al_2O_3	7.5% CO_2, 4.5% O_2, 15% H_2O, 73% N_2, 320 °C, 20 min	0.47	15% H_2/N_2, 320 °C, 1 h	0.18	[7]
10%Ni-6.1%"Na_2O"/Al_2O_3	7.5% CO_2, 4.5% O_2, 15% H_2O, 73% N_2, 320 °C, 20 min	0.11	15% H_2/N_2, 320 °C, 1 h	0.00	[7]
0.5%Ru-6.1%"Na_2O"/Al_2O_3	415 ppm CO_2, 20% O_2, 79% N_2, 320 °C, 45 min	0.2	15% H_2/N_2, 320 °C, 45 min	0.15	[8]
1% Ni/CeO_2-CaO (physically mixed)	15% CO_2/N_2, 550 °C, 60 min	15.3	100% H_2, 550 °C, 60 min	8.0	[9]
5%Ru/CeO_2-MgO (physically mixed)	65% CO_2/N_2, 300 °C, 60 min	4.25	5%H_2/N_2, 300 °C, 60 min	3.36	[10]
10%Ni-CaO	10% CO_2, 10% H_2O, 80% N_2, 500 °C, 120 min	8.96	90% H_2/N_2, 500 °C, 230 min	8.34	[11]
10%Ni-CaO	10% CO_2, 10% H_2O, 80% N_2, 600 °C, 120 min	15.49	90% H_2/N_2, 600 °C, 230 min	14.94	[11]
10%Ni-CaO	10% CO_2, 10% H_2O, 80% N_2, 700 °C, 120 min	16.22	90% H_2/N_2, 700 °C, 230 min	4.7	[11]

	Temperature-Swing Reactor Operating Conditions
	Isothermal Reactor Operating Conditions

References

1. C. Jeong-Potter, M. Abdallah, C. Sanderson, M. Goldman, R. Gupta and R. Farrauto, *Applied Catalysis B: Environmental*, 2021, **307**, 120990.
2. S. Wang, E. T. Schrunk and H. Mahajan, *Catalysts*, 2017, **7**, 88.
3. M. S. Duyar, M. A. A. Trevino and R. J. Farrauto, *Applied Catalysis B: Environmental*, 2015, **168**, 370-376.
4. Q. Zheng, R. Farrauto and A. Chau Nguyen, *Industrial & Engineering Chemistry Research*, 2016, **55**, 6768-6776.
5. M. S. Duyar, S. Wang, M. A. Arellano-Trevino and R. J. Farrauto, *Journal of CO_2 Utilization*, 2016, **15**, 65-71.
6. M. A. Arellano-Treviño, Z. He, M. C. Libby and R. J. Farrauto, *Journal of CO_2 Utilization*, 2019, **31**, 143-151.
7. M. A. Arellano-Treviño, N. Kanani, C. W. Jeong-Potter and R. J. Farrauto, *Chemical Engineering Journal*, 2019, **375**, 121953.
8. C. Jeong-Potter and R. Farrauto, *Applied Catalysis B: Environmental*, 2021, **282**, 119416.
9. H. Sun, Y. Wang, S. Xu, A. I. Osman, G. Stenning, J. Han, S. Sun, D. Rooney, P. T. Williams and F. Wang, *Fuel*, 2021, **286**, 119308.
10. H. Sun, Y. Zhang, S. Guan, J. Huang and C. Wu, *Journal of CO2 Utilization*, 2020, **38**, 262-272.
11. S. B. Jo, J. H. Woo, J. H. Lee, T. Y. Kim, H. I. Kang, S. C. Lee and J. C. Kim, *Sustainable Energy & Fuels*, 2020, **4**, 4679-4687.